

## Article

# Experimental Study on Microbial-Induced Calcium Carbonate Precipitation Repairing Fractured Rock under Different Temperatures

Junren Deng <sup>1</sup>, Hongwei Deng <sup>1,\*</sup>, Yanan Zhang <sup>2</sup> and Yilin Luo <sup>1</sup><sup>1</sup> School of Resources and Safety Engineering, Central South University, Changsha 410083, China<sup>2</sup> Department of Aerospace and Mechanical Engineering, University of Arizona, Tucson, AZ 85721, USA

\* Correspondence: 207010@csu.edu.cn

**Abstract:** Microbial-induced calcium carbonate precipitation (MICP) technology mainly uses carbonates produced by the reaction of microbial activities to repair rocks and soils. Temperature influences microbial metabolism and the kinetics of chemical reactions. In this study, microbial repair experiments on fractured sandstone under different temperatures are carried out. The repair effects are tested with nuclear magnetic resonance (NMR), an X-ray automatic diffractometer (XRD), uniaxial compressive strength (UCS), and a scanning electron microscope (SEM) test. The influence of the temperature on the restorative effects of MICP was discussed. The results show that the repair effect of the *Sporosarcina pasteurii* is significantly better as the temperature increases. When the temperature reaches 33 °C, the porosity and permeability of fractured sandstone can be reduced by 55.174% and 98.761%, respectively. The average uniaxial compressive strength can be restored to 6.24 MPa. The repair effect gradually weakens with the increase in temperature. However, the *Sporosarcina pasteurii* can still maintain relatively good biological activity at temperatures from 33 °C to 39 °C. The main form of CaCO<sub>3</sub> produced in the process of MICP is calcite. It can fill in the rock pores, and result in reducing the size and number of large pores and improving the impermeability and strength of fractured yellow sandstone.

**Keywords:** microbial mineralization; carbonate precipitation; rock fracture; rock strength



**Citation:** Deng, J.; Deng, H.; Zhang, Y.; Luo, Y. Experimental Study on Microbial-Induced Calcium Carbonate Precipitation Repairing Fractured Rock under Different Temperatures. *Sustainability* **2022**, *14*, 11770. <https://doi.org/10.3390/su141811770>

Academic Editor: Gianluca Mazzucco

Received: 16 August 2022

Accepted: 16 September 2022

Published: 19 September 2022

**Publisher's Note:** MDPI stays neutral with regard to jurisdictional claims in published maps and institutional affiliations.



**Copyright:** © 2022 by the authors. Licensee MDPI, Basel, Switzerland. This article is an open access article distributed under the terms and conditions of the Creative Commons Attribution (CC BY) license (<https://creativecommons.org/licenses/by/4.0/>).

## 1. Introduction

The durability problem of most rocks and building materials is the result of the combined effects of physical, chemical, biological, and other factors. Most problems are caused by external corrosive substances and water entering inside the material through pores and cracks on the surface of the material, resulting in the gradual degradation of the material from the inside to the outside. This often results in the entire structure being damaged before it reaches the expected service life. In addition, some underground engineering, such as underground reservoirs and oil depots, often has a higher requirement for the strength and impervious performance of rock mass. Concrete and chemical grouting materials are often used to improve strength and impervious performance. However, these materials have adverse effects on the environment because their production emits huge amounts of greenhouse gases, such as CO<sub>2</sub> [1–3]. Therefore, it is very urgent to study a new eco-friendly method to repair and reinforce damaged rock and building materials.

Microbial-induced calcium carbonate precipitation (MICP) remediation technology is a new remediation method, which mainly uses the products produced by microbial life activities to bind particles and fill material voids, thereby improving the strength and impermeability of materials. It is a biologically induced mineralization. This phenomenon was first discovered by Boquet et al. [3] in 1973, and this biologically induced mineralization exists widely in nature and often occurs in hot springs, oceans, and caves. The mineral crystals produced by biomineralization are diverse and involve diverse biological

processes and the environment [4–6]. The mineral formed by biomineralization generally has excellent repair characteristics. Even if the microorganisms are dead, their products still play a role for a long time. Biomineralization is a common form of calcium carbonate deposition in nature. Shrestha et al. [7] and Zhou et al. [8] thought that the process of depositing calcium carbonate can be achieved through four different types of reactions in nature: sulfate reduction, photosynthesis, denitrification, and urea hydrolysis.

MICP technology was first applied to porous media materials to reduce their permeability and increase their strength and rigidity [9]. Subsequently, this technology was applied to repair cracks on the surface of stone materials and cement-based materials [10]. Dejong et al. [1] conducted a MICP sand consolidation experiment, and revealed the migration and crystallization modes of microorganisms on sand particles. Later, the scale of the experiment was expanded to provide a feasible application prospect of biogeochemical MICP technology [11]. Minto et al. [12] compared the changes in the hydraulic properties of rock mass after microbial filling of micro-fractures, and found that the hydraulic aperture of the rock mass was significantly reduced after repair. Cuthbert et al. [13] fixed the ureolytic bacterium in the fractured rock, cementing fluid comprising  $\text{CaCl}_2$  and urea. The results show that MICP grouting induced the conductivity and permeability reduction of fractured rock surrounding the injection within 3 m by 35% and 99%, respectively. Phillips et al. [14] conducted field trials showing that MICP reduced the seepage velocity of fractured rocks by 25% and the permeability of artificially fractured rock samples by 80%. This suggests that MICP can be used to seal subsurface fractures in a near-wellbore environment. Deng et al. [15] and Gao et al. [16] used MICP to repair fractured rocks, and studied the effect of different repair times. After 42 days of repairing, the porosity of fractured sandstone decreases by 36.41%, the impermeability increases by 94.62%, and the compressive strength increases by 30.52%. Due to the simplicity and good filling effect, MICP remediation technology will be used more and more widely for seepage prevention in fractured rock masses [17].

Currently, the research on MICP mainly focuses on the influence of repair time. As underground resource development and engineering construction go deep, the environmental conditions of some deep engineering are obviously different from the surface. The temperature in the deep increases obviously. The research about temperature mainly focuses on the microbial culture stage [18,19]. However, the influence of temperature on the restoration effect of MICP is not clear.

In view of this, the MICP repair experiment was carried out on prefabricated fractured yellow sandstone. Quantitative analysis of the physical and mechanical properties after the experiment reveal the effect of temperature on the MICP repair effect of the fractured rock mass. The experimental results can provide a theoretical basis for its application in practice.

## 2. Materials and Methods

### 2.1. Bacteria Selection and Rock Sample Preparation

The urea hydrolysis has attracted much attention due to its advantages of a simple system, mild reaction conditions, easy control, and excellent environmental compatibility. Because of its strong enzyme-producing ability, non-pathogenicity, and ability to survive in harsh environments (such as high temperature and high salt), *Sporosarcina pasteurii* stands out from microorganisms that can secrete urease [20].

*Sporosarcina pasteurii* used in this study was purchased from the China General Microorganism Culture Collection Center (CGMCC) under the number ATCC<sup>®</sup> 11859<sup>™</sup>. It is an alkaliphilic bacteria abundant in soil. CGMCC provides this strain in the form of freeze-dried powder, which requires Casein Soyabean Digest Agar medium for activation.

Commonly used MICP treatment methods include grouting, soaking, spraying, and pre-stirring. Clayey rocks are easily softened and disintegrated in contact with water, which affects the restoration effect and is not suitable for this study. The highly alkaline environment inside materials such as concrete can inhibit the activity of *Sporosarcina pasteurii* and reduce the repair effect. The rock samples used in the experiment are yellow sandstone,

mainly composed of quartz and clay minerals. All rock samples were taken from intact and unweathered sandstone. According to the relevant standards [21], all rock samples were cut as standard cylinders with a diameter of  $(50 \pm 1)$  mm and a height of  $(100 \pm 1)$  mm. Afterwards, a water jet was used to produce an artificial crack with a length of 45 mm, a width of 5 mm, and an inclination angle of  $45^\circ$  in the middle of the cylindrical rock sample, as shown in Figure 1.



**Figure 1.** Prefabricated fractures in rock samples.

Generally, the production induced by microorganisms is used to cement the particles in the surrounding environment to form a cement with a certain strength and impermeability to achieve the expected repair effect. Therefore, more than 96%  $\text{SiO}_2$  and not more than 0.2% mud content (including soluble salts) were used for the filling aggregate. Before the start of the experiment, standard fine sand with a particle size of less than 0.3 mm was screened out.

## 2.2. Experimental Schemes

To reduce the error caused by the difference of rock samples, the wave velocity of the rock sample was tested with the HS-YS4A rock acoustic wave parameter tester. According to the test results of the rock samples, every three rock samples were taken as a group and numbered. A total of 5 experimental groups and 1 control group were set up. Group A was the control group and will not be repaired. Each experimental group corresponds to a repair temperature, and the repair temperature varies from  $27^\circ\text{C}$  to  $39^\circ\text{C}$  with an interval of  $3^\circ\text{C}$ . The grouping of the rock samples and the results of the acoustic wave test are shown in Table 1.

Before the experiment, all rock samples need to be vacuum saturated (vacuum pressure of 0.1 MPa and pumping time of 6 h). Then the specimens are tested by the AniMR-150 nuclear magnetic resonance imaging analysis system (NMR) to obtain the initial porosity. The initial permeability was obtained using the Coates model of the NMR analysis system [22].

Rock samples and quartz sand were disinfected in the drying oven (temperature  $105^\circ\text{C}$ , 48 h). The bacterial culture, liquid culture medium, and quartz sand were mixed evenly on the clean bench, and then filled into the prefabricated crack of the rocks. Each 50 g sand was mixed with 5 mL of bacterial culture and 5 mL culture medium. Rock samples were cultured in a constant temperature incubator, and then disinfected in a drying oven after repair (temperature  $105^\circ\text{C}$ , 48 h). Every 3 days, 5 mL of urea and  $\text{CaCl}_2$  with a concentration of 1 mol/L mixed solution and 5 mL of bacterial culture were slowly injected into the fracture to allow adequate penetration. The repair time of the rock sample was 21 days.

**Table 1.** Acoustic parameter of rock samples.

| Group and Number | Temperature (°C) | Height (mm) | Wave Speed ( $\times 10^3$ m/s) |
|------------------|------------------|-------------|---------------------------------|
| A1               | -                | 99.48       | 1.17                            |
| A2               |                  | 99.56       | 1.13                            |
| A3               |                  | 99.92       | 1.16                            |
| B1               | 27 °C            | 99.10       | 1.15                            |
| B2               |                  | 99.50       | 1.14                            |
| B3               |                  | 99.24       | 1.16                            |
| C1               | 30 °C            | 100.12      | 1.17                            |
| C2               |                  | 99.26       | 1.16                            |
| C3               |                  | 99.24       | 1.14                            |
| D1               | 33 °C            | 99.44       | 1.15                            |
| D2               |                  | 99.18       | 1.17                            |
| D3               |                  | 99.14       | 1.14                            |
| E1               | 36 °C            | 99.20       | 1.15                            |
| E2               |                  | 99.20       | 1.14                            |
| E3               |                  | 99.00       | 1.16                            |
| F1               | 39 °C            | 99.22       | 1.15                            |
| F2               |                  | 98.66       | 1.16                            |
| F3               |                  | 99.94       | 1.14                            |

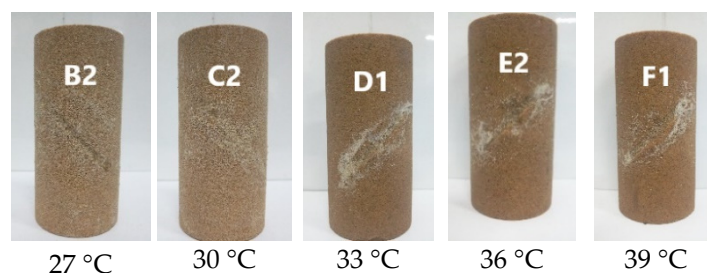
All the rock samples were saturated with water for NMR testing. After the NMR test, the rock samples were air-dried under room conditions for 3 days, and then the uniaxial compression strength (UCS) test was performed by the SHT4206 servo universal testing machine. The rock samples in the control group (group A) were directly subjected to UCS test without any repair. According to the stress–strain curve, the UCS and elastic modulus of rock samples were obtained [23]. The porosity, permeability, UCS, and elastic modulus of all rock samples were recorded.

Finally, we used an ADVANCE D8 X-ray automatic diffractometer (XRD) to analyze the composition of cemented sand in prefabricated fractures of repaired rock samples. The material filling the artificial cracks was extracted and observed in a Nova NanoSEM 230 Field Emission Scanning Electron Microscope (FESEM).

### 3. Results and Analysis

#### 3.1. Repairing Effect of MICP on the Surface

In order to observe the repair effect of MICP on the surface of fractured rock mass, the surface repair results from groups B to F were recorded. As shown in Figure 2, the prefabricated fissures of the rock sample are filled with a mixture of quartz sand. The quartz sand in the fractures is cemented together by the MICP products and sticks to the rock wall. After the repair, a large amount of visible white cement appeared in and around the fabricated crack.

**Figure 2.** Surface of the repaired rock samples.

It is obvious that the amount of white cement attached to the fabricated fractures of group D (33 °C) rock samples is the largest. When the ambient temperature is lower or

higher than 33 °C, the amount of white cement around the fabricated fractures decreases to varying degrees. It indicates that the repair effect of *Sporosarcina pasteurii* is the best when the ambient temperature is 33 °C. The amounts of white cement around the prefabricated fractures of the rock samples in groups E (36 °C) and F (39 °C) are larger than that of groups B (27 °C) and C (30 °C). This shows that *Sporosarcina pasteurii* can maintain relatively good repair activity when the ambient temperature is above 33 °C.

### 3.2. Repairing Effect of MICP on Permeability and Porosity

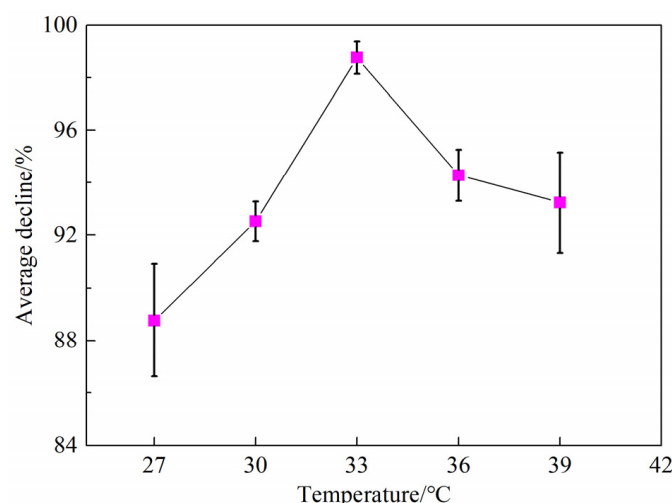
The permeability and porosity are two important parameters to evaluate the seepage characteristics of rock materials. In this experiment, these two parameters of the repaired rock sample are evaluated using NMR with the Coates model [22].

Table 2 lists the permeability of the rock samples before and after repair. Before MICP repair treatment, the permeability of rock samples was in the range of 80–120 mD. After MICP repair treatment, the permeability of each group of rock samples decreased dramatically. When the ambient temperature exceeds 30 °C, the permeability of all repaired rock samples drops below 10 mD. The permeability of rock samples generally dropped by one or two ratings, and turned into a type of rock with poor permeability. It shows that the cementation of MICP products in the internal pore structure of the rock sample effectively improves the anti-permeability performance of the rock mass.

**Table 2.** Permeability variation of rock samples.

| Number | Temperature (°C) | Pre-Repair Permeability (mD) | Post-Repair Permeability (mD) | Average Decline (%) |
|--------|------------------|------------------------------|-------------------------------|---------------------|
| A1     | -                | 111.579                      |                               |                     |
| A2     |                  | 102.797                      |                               |                     |
| A3     |                  | 115.589                      |                               |                     |
| B1     | 27 °C            | 109.655                      | 14.135                        | 88.768              |
| B2     |                  | 117.008                      | 9.968                         |                     |
| B3     |                  | 92.107                       | 11.317                        |                     |
| C1     | 30 °C            | 101.053                      | 7.29                          | 92.517              |
| C2     |                  | 81.089                       | 6.757                         |                     |
| C3     |                  | 90.896                       | 6.274                         |                     |
| D1     | 33 °C            | 116.833                      | 2.051                         | 98.761              |
| D2     |                  | 113.074                      | 0.635                         |                     |
| D3     |                  | 114.834                      | 1.609                         |                     |
| E1     | 36 °C            | 111.3                        | 5.298                         | 94.274              |
| E2     |                  | 101.607                      | 5.807                         |                     |
| E3     |                  | 92.579                       | 6.206                         |                     |
| F1     | 39 °C            | 94.823                       | 5.136                         | 93.233              |
| F2     |                  | 109.511                      | 6.352                         |                     |
| F3     |                  | 95.22                        | 8.649                         |                     |

Figure 3 shows the average decline rate of permeability with different repair temperatures. When the ambient temperature is in the range of 27–33 °C, the average decline rate of permeability of the repaired rock sample increases with the increase in temperature, and the decline rate reaches the maximum value of 98.761% when the temperature increases to 33 °C. Then, as the temperature increased to 36 °C, the permeability of the repaired rock sample decreased by 94.274%. When the temperature is 39 °C, it dropped by 93.233%. It is still higher than 92.517% when the temperature is 30 °C. This indicated that the optimum temperature for MICP repair of rocks using *Sporosarcina pasteurii* is around 33 °C. When the temperature is above 33 °C, *Sporosarcina pasteurii* can reduce the permeability of rock material within a temperature range used in this study.



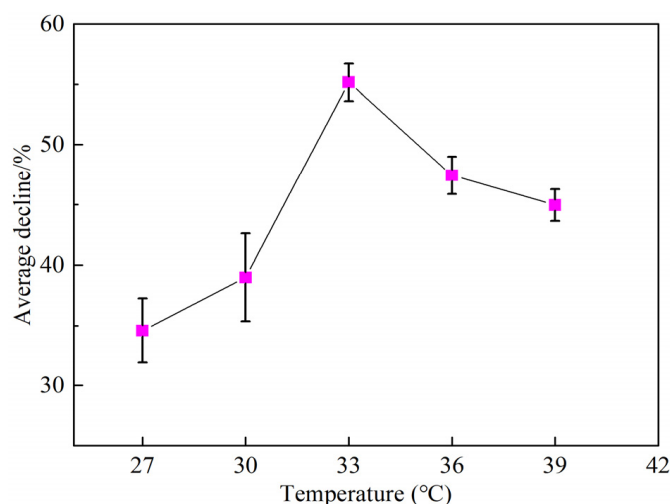
**Figure 3.** Permeability variation of rock samples at different temperatures.

Table 3 and Figure 4 shows the average porosity and its decline rate with different repair temperatures. It can be seen that the overall average porosity of the repaired rock samples shows a minimum value of 7.404% at 33 °C, which is 55.174% lower than that before repairing.

**Table 3.** Porosity variation of rock samples.

| Number | Temperature (°C) | Pre-Repair Porosity (%) | Post-Repair Porosity (%) | Average Decline (%) |
|--------|------------------|-------------------------|--------------------------|---------------------|
| A1     |                  | 16.482                  |                          |                     |
| A2     | -                | 16.571                  |                          |                     |
| A3     |                  | 17.129                  |                          |                     |
| B1     |                  | 15.538                  | 10.631                   |                     |
| B2     | 27 °C            | 16.131                  | 10.213                   | 34.582              |
| B3     |                  | 15.787                  | 10.186                   |                     |
| C1     |                  | 15.671                  | 9.433                    |                     |
| C2     | 30 °C            | 15.320                  | 9.956                    | 38.978              |
| C3     |                  | 16.118                  | 9.330                    |                     |
| D1     |                  | 16.570                  | 7.516                    |                     |
| D2     | 33 °C            | 16.508                  | 7.109                    | 55.174              |
| D3     |                  | 16.472                  | 7.586                    |                     |
| E1     |                  | 16.555                  | 8.918                    |                     |
| E2     | 36 °C            | 16.401                  | 8.695                    | 47.425              |
| E3     |                  | 15.657                  | 7.960                    |                     |
| F1     |                  | 16.208                  | 9.086                    |                     |
| F2     | 39 °C            | 16.829                  | 9.013                    | 44.954              |
| F3     |                  | 16.460                  | 9.139                    |                     |

Similar to the change trend of permeability, the porosity of all rock samples decreased after MICP repair. When the temperature was 36 °C and 39 °C, the porosity of the repaired rock samples decreased by 47.425% and 44.954%, respectively, which still are higher than the drop of 38.978% at 27 °C. This also indicated that *Sporosarcina pasteurii* could reduce the porosity in the temperature range used in this study.



**Figure 4.** Porosity variation of rock samples at different temperatures.

### 3.3. Effect of MICP on UCS of Fractured Rock Samples

Table 4 and Figure 5 shows the UCS and elasticity modulus of rock samples repaired at different temperatures. For all temperatures, the UCS and elasticity modulus have been improved after the MICP restoration treatment. The change trend of the average UCS of the repaired rock sample is similar to that of the elasticity modulus. The UCS and elasticity modulus reach the maximum 6.24 MPa and 15.565 GPa at a temperature of 33 °C, respectively. When the temperature is above 33 °C, both UCS and elasticity modulus decrease with increasing temperature. Figure 6 also shows that the UCS and elasticity modulus of the rock samples of groups E (36 °C) and F (39 °C) are higher than that of group C (30 °C). This is in line with the trend of permeability differences observed in Table 2 and Figure 3.

**Table 4.** UCS and Elasticity modulus of repaired rock samples.

| Number | Temperature (°C) | UCS (MPa) | Elasticity Modulus (GPa) |
|--------|------------------|-----------|--------------------------|
| A1     |                  | 3.18      | 6.907                    |
| A2     | -                | 3.09      | 6.096                    |
| A3     |                  | 3.41      | 6.267                    |
| B1     |                  | 4.354     | 6.922                    |
| B2     | 27 °C            | 4.25      | 7.403                    |
| B3     |                  | 4.522     | 7.919                    |
| C1     |                  | 4.869     | 9.913                    |
| C2     | 30 °C            | 5.095     | 11.524                   |
| C3     |                  | 4.785     | 10.477                   |
| D1     |                  | 6.229     | 15.943                   |
| D2     | 33 °C            | 6.379     | 15.896                   |
| D3     |                  | 6.112     | 14.855                   |
| E1     |                  | 5.769     | 13.695                   |
| E2     | 36 °C            | 5.782     | 12.807                   |
| E3     |                  | 6.016     | 13.979                   |
| F1     |                  | 5.697     | 11.558                   |
| F2     | 39 °C            | 5.629     | 12.100                   |
| F3     |                  | 5.556     | 11.817                   |

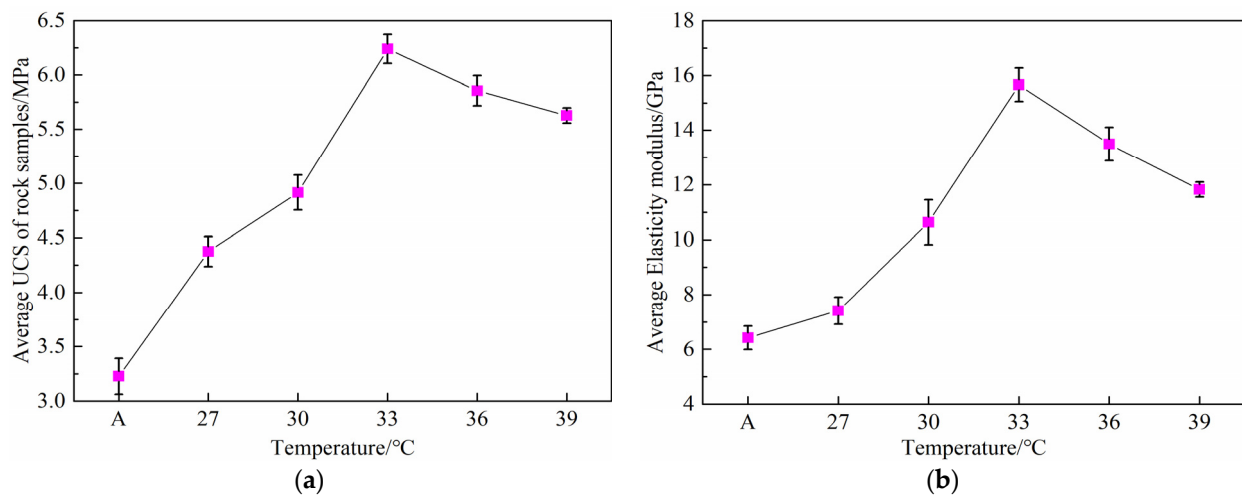


**Figure 5.** Average UCS and elasticity modulus of rock samples; (a) Average UCS; (b) Average elasticity modulus.

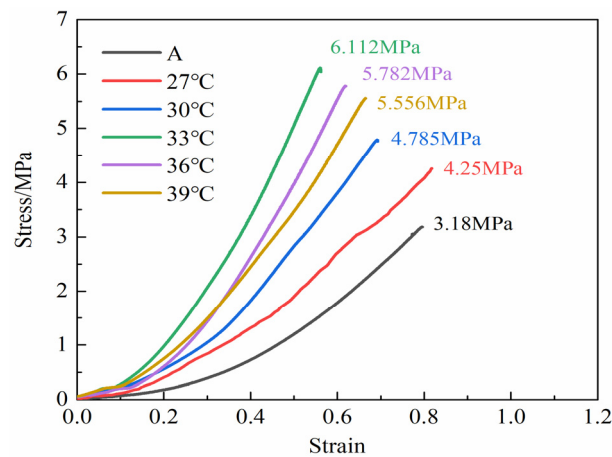


**Figure 6.** Stress-strain curves of rock samples repaired at different temperatures.

Figure 6 shows the typical stress–strain curves of rock samples repaired at different temperatures. Compared with the unrepaired rock sample, the micro-crack compaction stage of the repaired rock sample has shifted to the left in varying degrees. This indicates that the MICP products cemented the quartz sand in the fracture, and the formed cement effectively filled the fracture, making the rock sample enter the elastic deformation stage earlier. In addition, MICP products fill the micro-cracks, improve the rock’s resistance to stress, and remedy internal defects.

The above results show that when the temperature is 33 °C, MICP has the best effect of repairing prefabricated fractured yellow sandstone. In practical applications, it is generally difficult to reach or maintain 33–39 °C for a long time, so some measures of heat preservation or temperature increase need to be taken. We can apply thermal insulation film before entering the night, but the film needs to be removed regularly to ensure sufficient oxygen supply. In addition, artificial measures such as furnace heating and electric heating wire heating can be used to increase the temperature, and pipelines can be used to ensure that the repaired area is heated evenly.

#### 4. Discussion

According to the results, it can be found that temperature has an important influence on the restoration effect of MICP restoration of fractured rock. However, analyzing the effect of temperature on the remediation effect of MICP from changes in permeability, porosity, and UCS alone is not enough to fully understand the remediation process.

#### 4.1. Influence of Temperature on Biological Activity

The *Sporosarcina pasteurii* used in this study uses urea as an energy source to produce highly active urease through the process of metabolism to catalyze the hydrolysis of urea [24], which hydrolyzes urea to  $\text{NH}_4^+$  and  $\text{CO}_3^{2-}$ . During this process, the extracellular polymeric substances (EPS) secreted by bacteria will continuously adsorb  $\text{Ca}^{2+}$ . *Sporosarcina pasteurii* increases the alkalinity of the surrounding environment through its own metabolic activities, and  $\text{Ca}^{2+}$  and  $\text{CO}_3^{2-}$  will combine to form  $\text{CaCO}_3$  crystals [25]. The entire reaction process is shown in Formula (1)



Based on the experimental results, the temperature has an important influence on the biological activity of *Sporosarcina pasteurii*. When the ambient temperature is 33 °C, the biological activity of *Sporosarcina pasteurii* is the highest. During this temperature, the *Sporosarcina pasteurii* is easier to reproduce and carry out life activities. When the ambient temperature is higher than 33 °C, *Sporosarcina pasteurii* can still maintain relatively superior biological activity. The production induced by the *Sporosarcina pasteurii* is pretty less when the ambient temperature less than 30 °C, and the biological activity of *Sporosarcina pasteurii* is lower.

Previous studies have shown that the optimum temperature for catalytic activity of pure urease solution is 50 °C, and the temperature of the highest urease activity in soil is 60–70 °C [26,27]. In this study, fractured rock samples were repaired by using the bacterial culture rather than the pure solution of urease. This indicates that urea hydrolysis is only a part of the MICP process. The  $\text{CaCO}_3$  precipitation generated by bacterial mineralization is not directly generated by the decomposition of substrates by extracellular enzymes, but requires the participation of the living bacteria. When the ambient temperature exceeds the appropriate range, the bacterial activity is inhibited, which in turn leads to a decrease in the MICP repair efficiency.

#### 4.2. Microscopic Analysis of MICP Products

Figure 7 shows the XRD pattern of the mixture in the prefabricated fractures of the repaired rock samples detected obvious  $\text{SiO}_2$  peaks and  $\text{CaCO}_3$  peaks. According to the XRD characterization of common rock minerals, it can be determined that the crystal phase of the generated  $\text{CaCO}_3$  is mainly calcite. The tested production is same as the predicted results in the Equation (1).

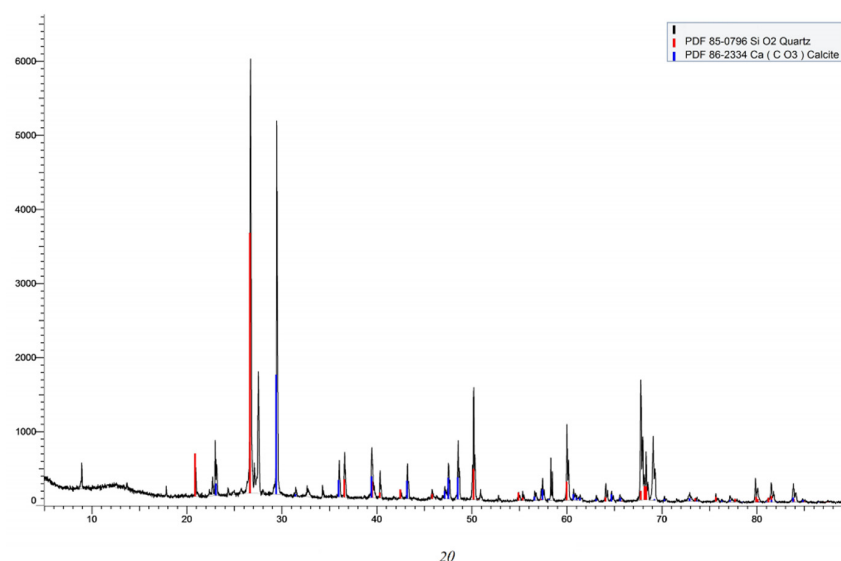
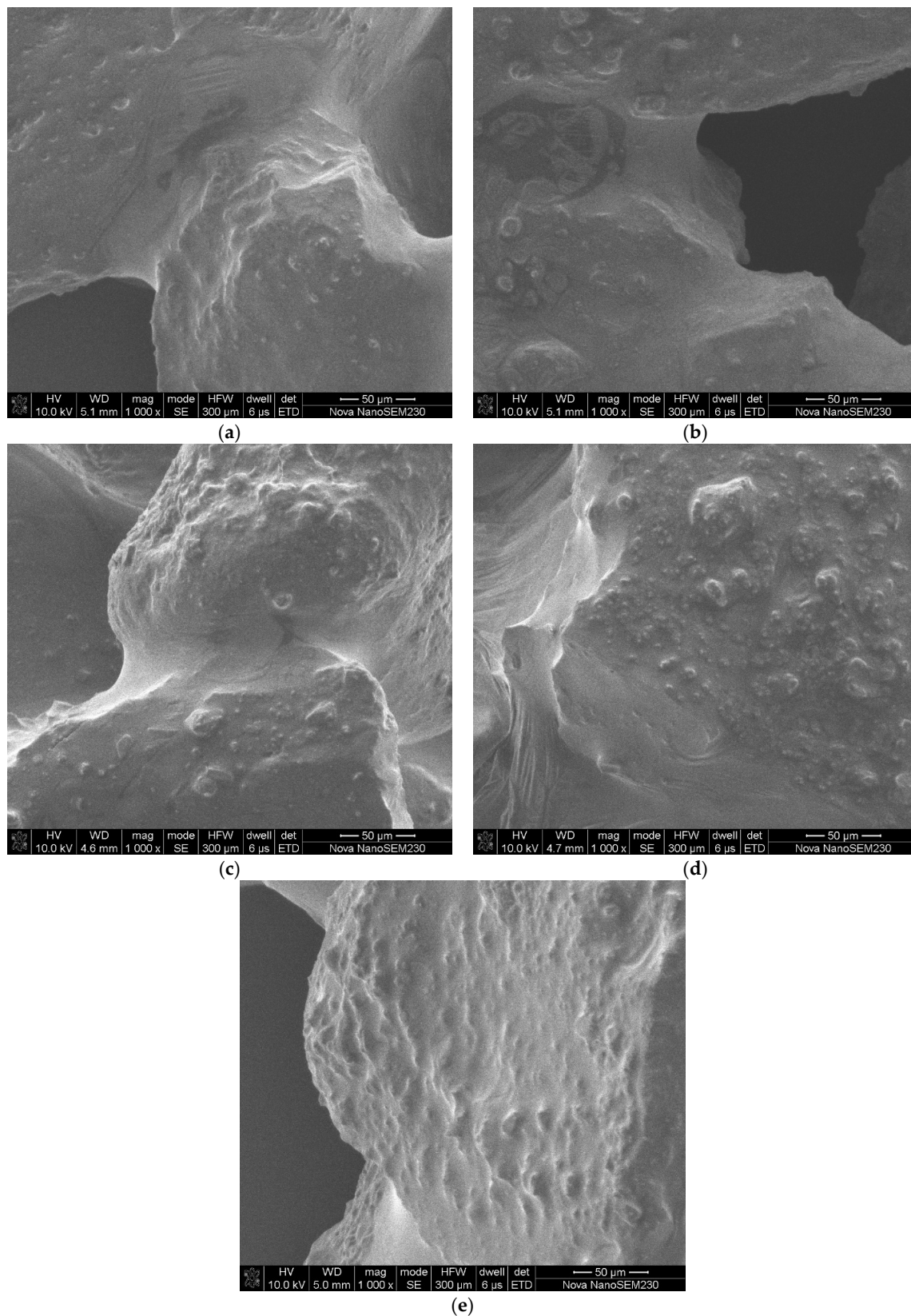


Figure 7. XRD test results of the repaired products of group D (33 °C).

The mesoscopic structure of the cement was obtained by scanning electron microscopy (SEM), as shown in Figure 8.



**Figure 8.** SEM microscopic images of  $\text{CaCO}_3$  among sand particles in samples incubated at different temperatures: (a) 27 °C; (b) 30 °C; (c) 33 °C; (d) 36 °C; (e) 39 °C.

It can be seen from Figure 8 that the  $\text{CaCO}_3$  formed during the repair process has two distribution modes. One mode is the  $\text{CaCO}_3$  crystals formed on the surface of the sand increases the grain size. The other is the  $\text{CaCO}_3$  crystals deposited between sand grains, cementing them to each other and with the rock.

#### 4.3. Influence of Temperature on the Composition and Morphology of Cement

As the  $\text{CaCO}_3$  produced by MICP is deposited in the internal pores of the sandstone, or the quartz sand within fabricated fractures is cemented by  $\text{CaCO}_3$ , the pore structure inside the rock sample will be affected. With different repair temperatures, the distribution of the pore structure is different. Based on the NMR test result, the distribution of the pore structure can be calculated with the T2 spectral distribution curve.

Referring to the work of Deng et al. [28] and Lin et al. [29], pores with a transversal relaxation time of less than 10 ms are defined as micropores, those between 10 and 100 ms are defined as mesopores, and those over 100 ms are defined as macropores.

Figure 9 shows the comparison of the three types of pores between the unrepaired and repaired rock. After repair, the proportion of large pores in the rock sample decreases, while the proportion of small pores increases. The results indicate that as  $\text{CaCO}_3$  cements and deposits in the pores of the rock sample, the original space of the pores is blocked, and the pore size of the inner pores of the rock sample decreases. Some large pores are transformed into medium pores and small pores, the size and number of large pores are reduced, and the homogeneity of the rock sample increases.

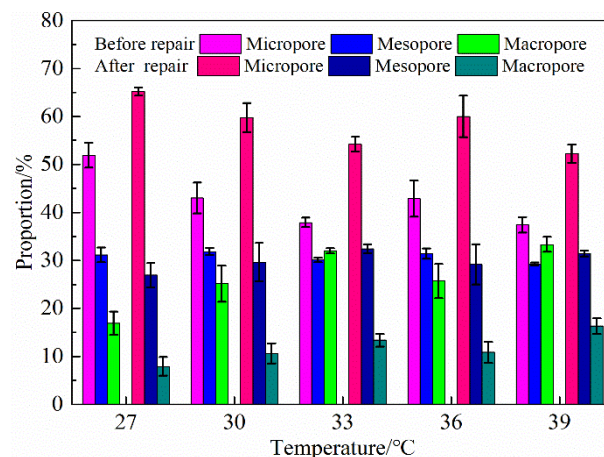


Figure 9. Average proportion of pores with different pore sizes before and after MICP treatment.

The average proportion of micropores increased from 37.89% to 54.21%, and the average proportion of macropores decreased from 32.01% to 13.38% when the temperature is 33 °C. The rate of micropores proportion increased by 43.08%, and the rate of macropores proportion decreased by 58.2%, both of which were the maximum values of each group of rock samples.

## 5. Conclusions

MICP is a new type of eco-friendly repair and reinforcement technology to improve the strength and impervious performance for rock and building materials. In this study, the MICP restoration experiments using *Sporosarcina pasteurii* with different repair temperatures are conducted for fractured yellow sandstone. The influence of the temperature on the repair effect and repair mechanism are analyzed. The main conclusions are as follows.

1. The optimum temperature for *Sporosarcina pasteurii* to repair the fractured yellow sandstone is about 33 °C. The repair effect between 33 °C and 39 °C is better than between 27 °C and 30 °C.

2. The MICP can effectively improve impermeability and strength. At the optimum temperature, the permeability and porosity of repaired fractured yellow sandstone are reduced by 98.761% and 55.174%, respectively. The average uniaxial compressive strength is restored to 6.24 MPa.
3. The main form of CaCO<sub>3</sub> crystals produced in the process of MICP is calcite. At 33 °C, the deposition of CaCO<sub>3</sub> minerals is the highest. The CaCO<sub>3</sub> crystals fill in the pore of rock, reducing the size and number of large pores and decreasing the permeability and strength of fractured yellow sandstone.

**Author Contributions:** Conceptualization, H.D.; methodology, J.D.; validation, J.D., Y.Z. and Y.L.; formal analysis, J.D. and Y.Z.; data curation, Y.L.; writing—original draft preparation, J.D.; writing—review and editing, Y.Z. and H.D.; visualization, J.D.; supervision, H.D.; project administration, H.D.; funding acquisition, Y.L. All authors have read and agreed to the published version of the manuscript.

**Funding:** This research was supported by the National Natural Science Foundation of China (grant No. 51874352).

**Institutional Review Board Statement:** Not applicable.

**Informed Consent Statement:** Not applicable.

**Data Availability Statement:** The data presented in this study are available upon reasonable request from the corresponding author.

**Conflicts of Interest:** The authors have no conflict of interest to declare.

## References

1. DeJong, J.T.; Mortensen, B.M.; Martinez, B.C.; Nelson, D.C. Bio-mediated soil improvement. *Ecol. Eng.* **2010**, *36*, 197–210. [[CrossRef](#)]
2. Karol, R.H. *Chemical Grouting and Soil Stabilization*; Marcel Dekker: New York, NY, USA, 2003.
3. Boquet, E.; Boronat, A.; Ramos-Cormenzana, A. Production of calcite (calcium carbonate) crystals by bacteria is a common phenomenon. *Nature* **1973**, *45*, 527. [[CrossRef](#)]
4. Seifan, M.; Samani, A.K.; Berenjian, A. A novel approach to accelerate bacterially induced calcium carbonate precipitation using oxygen releasing compounds (ORCs). *Biocatal. Agric. Biotechnol.* **2017**, *12*, 299–307. [[CrossRef](#)]
5. Lowenstam, H.A.; Margulis, L. Evolutionary prerequisites for early phanerozoic calcareous skeletons. *Biosystems* **1980**, *12*, 27–41. [[CrossRef](#)]
6. Lowenstam, H.A. Minerals formed by organisms. *Science* **1981**, *211*, 1126–1131. [[CrossRef](#)]
7. Shrestha, P.; Gautam, R.; Ashwath, N. Effects of agronomic treatments on functional diversity of soil microbial community and microbial activity in a revegetated coal mine spoil. *Geoderma* **2019**, *338*, 40–47. [[CrossRef](#)]
8. Zhou, J.; Chen, D.; Huang, R.; Huang, G.; Yuan, Y.; Fan, H. Effects of bacterial-feeding nematodes on soil microbial activity and the microbial community in oil-contaminated soil. *J. Environ. Manag.* **2019**, *234*, 424–430. [[CrossRef](#)]
9. Van Passen, L.A.; Daza, C.M.; Staal, M.; Sorokin, D.Y.; van der Zon, W.; van Loosdrecht, M.C.M. Potential soil reinforcement by biological denitrification. *Ecol. Eng.* **2010**, *36*, 168–175. [[CrossRef](#)]
10. Qian, C.X.; Ren, L.F.; Luo, M. Development of Concrete Surface Defects and Cracks Repair Technology Based on Microbial-Induced Mineralization. *J. Chin. Ceram. Soc.* **2015**, *43*, 619–631. [[CrossRef](#)]
11. Dejong, J.T.; Soga, K.; Banwart, S.A.; Whalley, W.R.; Ginn, T.R.; Nelson, D.C.; Mortensen, B.M.; Martinez, B.C.; Barkouki, T. Soil engineering in vivo: Harnessing natural biogeochemical systems for sustainable, multi-functional engineering solutions. *J. R. Soc. Interface* **2011**, *8*, 1–15. [[CrossRef](#)]
12. Minto, J.; MacLachlan, E.; El Mountassir, G.; Lunn, R.J. Rock fracture grouting with microbially induced carbonate precipitation. *Water Resour. Res.* **2016**, *52*, 8827–8844. [[CrossRef](#)]
13. Cuthbert, M.O.; Mcmillan, L.A.; Handley-Sidhu, S.; Riley, M.S.; Tobler, D.J.; Phoenix, V.R. A field and modeling study of fractured rock permeability reduction using microbially induced calcite precipitation. *Environ. Sci. Technol.* **2013**, *47*, 13637–13643. [[CrossRef](#)] [[PubMed](#)]
14. Phillips, A.J.; Cunningham, A.B.; Gerlach, R.; Hiebert, R.; Hwang, C.; Lomans, B.P. Fracture Sealing with Microbially-induced Calcium Carbonate Precipitation: A Field Study. *Environ. Sci. Technol.* **2016**, *50*, 4111–4117. [[CrossRef](#)] [[PubMed](#)]
15. Deng, H.W.; Luo, Y.L.; Deng, J.R.; Wu, L.J.; Zhang, Y.N.; Peng, S.Q. Experimental study of improving impermeability and strength of fractured rock by microbial induced carbonate precipitation. *Rock Soil Mech.* **2019**, *40*, 3542–3548. [[CrossRef](#)]
16. Gao, R.; Luo, Y.; Deng, H. Experimental study on repair of fractured rock mass by microbial induction technology. *R. Soc. Open Sci.* **2019**, *6*, 191318. [[CrossRef](#)]

17. Liu, D.; Shao, A.L.; Jin, C.Y.; Yan, L. Healing technique for rock cracks based on Microbiologically Induced Calcium Carbonate mineralization. *J. Mater. Civ. Eng.* **2018**, *30*, 82–86. [[CrossRef](#)]
18. Liang, C.; Shahin, M.A.; Mujah, D. Influence of Key Environmental Conditions on Microbially Induced Cementation for Soil Stabilization. *J. Geotech. Geoenviron. Eng.* **2017**, *143*, 04016083. [[CrossRef](#)]
19. Sun, X.H.; Miao, L.C.; Tong, T.Z.; Wang, C.C. Study of the effect of temperature on microbially induced carbonate precipitation. *Acta Geotech.* **2018**, *14*, 627–638. [[CrossRef](#)]
20. Omoregie, A.I.; Khoshdelnezamiha, G.; Senian, N.; Ong, D.E.L.; Nissom, P.M. Experimental optimisation of various cultural conditions on urease activity for isolated *Sporosarcina pasteurii* strains and evaluation of their biocement potentials. *Ecol. Eng.* **2017**, *109*, 65–75. [[CrossRef](#)]
21. SL264-2001. Specifications for Rock Tests in Water Conservancy and Hydroelectric Engineering. China Water & Power Press: Beijing, China, 2001.
22. Coates, G.R.; Peveraro, R.C.A.; Hardwick, A.; Roberts, D. The Magnetic Resonance Imaging Log Characterized by Comparison with Petrophysical Properties and Laboratory Core Data. In Proceedings of the SPE Annual Technical Conference and Exhibition, Dallas, TX, USA, 6–9 October 1991. [[CrossRef](#)]
23. Huang, Y.H.; Yang, S.Q.; Ranjith, P.G.; Zhao, J. Strength failure behavior and crack evolution mechanism of granite containing pre-existing non-coplanar holes: Experimental study and particle flow modeling. *Comput. Geotech.* **2017**, *88*, 182–198. [[CrossRef](#)]
24. Wang, J.Y.; Snoeck, D.; Van Vlierberghe, S.; Verstraete, W.; Belie, N.D. Application of hydrogel encapsulated carbonate precipitating bacteria for approaching a realistic self-healing in concrete. *Constr. Build. Mater.* **2014**, *68*, 110–119. [[CrossRef](#)]
25. Jonkers, H.M.; Thijssen, A.; Muyzer, G.; Copuroglu, O.; Schlangen, E. Application of bacteria as self-healing agent for the development of sustainable concrete. *Ecol. Eng.* **2010**, *36*, 230–235. [[CrossRef](#)]
26. Moyo, C.C.; Kissel, D.E.; Cabrera, M.L. Temperature effects in soil urease activity. *Soil Biol. Biochem.* **1989**, *21*, 935–938. [[CrossRef](#)]
27. Guan, S.Y. *Soil Enzymes and Their Research Methods*; China Agricultural Publishing House: Beijing, China, 1987.
28. Deng, H.W.; Liu, C.J.; Ke, B.; Wang, Y.; Zhang, Y.N. Experimental study on microscopic damage characteristics of granite under cyclic dynamic disturbances. *Chin. J. Eng.* **2017**, *39*, 1634–1639. [[CrossRef](#)]
29. Lin, Y.; Zhou, K.P.; Gao, R.G.; Li, J.L.; Zhang, J. Influence of Chemical Corrosion on Pore Structure and Mechanical Properties of Sandstone. *Geofluids* **2019**, *2019*, 7320536. [[CrossRef](#)]